

## Ligand Exchange Processes on Solvated Lithium Cations. II. Complexation by Cryptands in $\gamma$ -Butyrolactone as Solvent

EWA PASGRETA<sup>1</sup>, RALPH PUCHTA<sup>1,2</sup>, MICHAEL GALLE<sup>1,2</sup>,  
NICO VAN EIKEMA HOMMES<sup>2</sup>, ACHIM ZAHL<sup>1</sup> and RUDI VAN ELDIK<sup>1,\*</sup>

<sup>1</sup>Institute for Inorganic Chemistry, University of Erlangen-Nürnberg, Egerlandstr.1, 91058, Erlangen, Germany;

<sup>2</sup>Computer Chemistry Center, University of Erlangen-Nürnberg, Nögelsbachstr. 25, 91052, Erlangen, Germany

(Received: 14 April 2006; in final form: 29 May 2006)

**Key words:**  $\gamma$ -butyrolactone, cryptands, exchange mechanism, Lithium

### Abstract

Kinetic studies on  $\text{Li}^+$  exchange between the cryptands C222 and C221, and  $\gamma$ -butyrolactone as solvent were performed as a function of ligand-to-metal ratio, temperature and pressure using  $^7\text{Li}$  NMR. The thermal rate and activation parameters are: C222:  $k_{298} = (3.3 \pm 0.8) \times 10^4 \text{ M}^{-1} \text{ s}^{-1}$ ,  $\Delta H^\ddagger = 35 \pm 1 \text{ kJ mol}^{-1}$  and  $\Delta S^\ddagger = -41 \pm 3 \text{ J K}^{-1} \text{ mol}^{-1}$ ; C221:  $k_{298} = 105 \pm 32 \text{ M}^{-1} \text{ s}^{-1}$ ,  $\Delta H^\ddagger = 48 \pm 1 \text{ kJ mol}^{-1}$  and  $\Delta S^\ddagger = -45 \pm 2 \text{ J K}^{-1} \text{ mol}^{-1}$ . Temperature and pressure dependence measurements were performed in the presence of an excess of  $\text{Li}^+$ . The influence of pressure on the exchange rate is insignificant for both ligands, such that the value of activation volume is around zero within the experimental error limits. The activation parameters obtained in this study indicate that the exchange of  $\text{Li}^+$  between solvated and chelated  $\text{Li}^+$  ions follows an associative interchange mechanism.

### Introduction

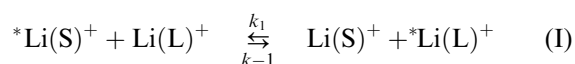
Following the work of Pedersen on two-dimensional crowns, Lehn and coworkers developed in 1969 a range of three-dimensional, polycyclic ligand systems, which they named cryptands (Greek: *cryptos* = cave) [1, 2]. Until today this class of compounds has been intensively explored and extended in different directions [3, 4] in terms of cavity size [5, 6], donor atoms [7], and metallatopomers [8–11]. Since cryptands readily form complexes with a wide range of metal ions and  $\text{NH}_4^+$  [12], provided the ion involved is not too large to be contained in the macrocyclic cavity [13], they find their application in various areas like catalysis, medicine, biomimetic research [14–21], and as receptors [22] and electrified [23]. Studies on the complexes (cryptates) formed between alkali metal ions and cryptands, have revealed a substantial understanding of the effects of metal ion size and cryptand cavity size on the structure, stability and lability of cryptates, and the mechanism of the cryptate complex-formation processes [24–28]. Such selective complexation has led to many biological and chemical studies.

Kinetic studies on macrocyclic complex-formation reactions with alkali cations not only result in important information on the rates and mechanisms of complex-formation reactions, but also lead to a better understanding of the high selectivity of these ligands toward

different cations. The broad impact of such studies spans from the theory of complexation to cation transport through membranes, and makes the ability to control cation selectivity via tactical structural changes in the complexing agent of prime importance [18]. Polyoxo macrobicyclic diamines, represented by the structure in Figure 1, are able to form metal ion complexes in which the metal ion is located in the cavity of the macromolecule and two nitrogen atoms along with the oxygen atoms participate in binding the metal cation. All complexes have 1:1 stoichiometry with the metal ion positioned in the center of the ligand cavity [24].

In case of crown ethers and cryptands in non-aqueous solutions, the rates of complex-formation ( $k_f$ ) for the interaction with alkali-metal cations are generally diffusion-controlled and, consequently, the complexation selectivities are governed by the decomplexation rates  $k_d$  [29]. These reactions have received significant attention, initially from Lehn and co-workers and more recently from Popov and co-authors [30–32] and Lincoln and co-authors [33–40]. These and other groups performed a series of detailed kinetic studies and found that two mechanisms need to be considered for the decomplexation process of cryptand-alkali metal cation complexes, viz., bimolecular associative (I) and unimolecular dissociative (back reaction in II) cation exchange processes, where S presents solvent and L the employed chelate [41, 42].

\* Author for correspondence. E-mail: vaneldik@chemie.uni-erlangen.de



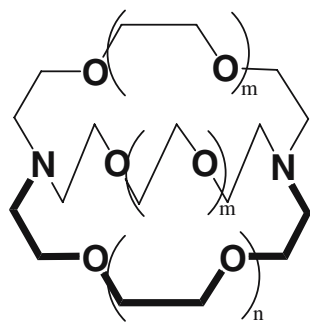
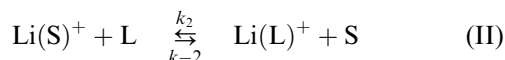


Figure 1. Chelate structures. C211:  $m = 0$ ,  $n = 1$ . C221:  $m = 1$ ,  $n = 0$ . C222:  $m = 1$ ,  $n = 1$ .



The solvent plays a major role in the unimolecular mechanism II [43, 44], which is therefore favored in strong donor solvents. Many examples have been included in a series of review articles [41, 45–47]. It has been reported that ligand structure and solvent properties have considerable effects on the reaction rates, activation parameters, and exchange mechanism of cations between the solvated and complexed sites. We have now extended the study of  $\text{Li}^+$  exchange to  $\gamma$ -butyrolactone (see Figure 2) as solvent.

$\gamma$ -Butyrolactone was chosen as solvent due to its relevance in lithium batteries and capacitors [48, 49]. It is a model cyclic ester used as a major chemical compound with extensive application in pharmaceuticals, pesticides and petrochemicals. The butyrolactone ring is an integral building block of many natural products of biological activity [50, 51], like the sesquiterpene lactones, flavor components, alkaloids, antileukemics, and pheromones.  $\gamma$ -Butyrolactone is one of the important intermediates in fine chemical industrial practices, for example in the synthesis of pyrrolidine, herbicides and rubber additives [52]. It is also used as a solvent for surface treatment of textiles and metal coated plastics, as a paint remover, in photochemical etching, in vitamin and pharmaceutical preparations.

Recently, computational studies on  $\gamma$ -butyrolactone and  $\text{Li}^+/\gamma$ -butyrolactone have been performed by Rey and co-author [53]. It was found that the  $\text{Li}^+$  cation coordinates to the carbonyl oxygen with an almost colinear configuration relative to the carbon-oxygen bond but with a slight tilting toward the lactone oxygen. This configuration holds for clusters of up to four molecules and also in the liquid phase, where a tetrahedral first solvation (coordination) sphere was found.

In this contribution, we report kinetic parameters for the exchange of  $\text{Li}^+$  in  $\gamma$ -butyrolactone under ambient and elevated pressure conditions, and discuss their mechanistic implications.

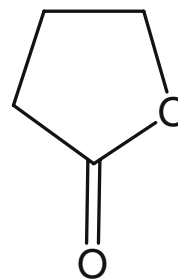


Figure 2. Structure of  $\gamma$ -butyrolactone.

## Experimental section

### General procedures

The preparation of test solutions was carried out under an Ar or  $\text{N}_2$  atmosphere using standard Schlenk techniques, under an Ar atmosphere in a glove box, or under vacuum. Lithium perchlorate (Aldrich, battery grade) was vacuum-dried at  $120^\circ\text{C}$  for 48 h and then stored under dry nitrogen. The cryptands C222 (purchased from Fluka), C221 and C211 (purchased from Aldrich) were dried under vacuum for 48 h and stored under dry nitrogen.  $\gamma$ -Butyrolactone (Aldrich) was dried over anhydrous  $\text{CaSO}_4$ , then fractionally distilled under vacuum and stored under nitrogen over Linde 3 Å molecular sieves. Solutions of  $\text{LiClO}_4$ , C222, C221 and C211 in  $\gamma$ -butyrolactone were prepared under dry nitrogen. For the  $^7\text{Li}$  NMR measurements the solutions were sealed in 5 mm NMR tubes under an Ar atmosphere. In order to study the kinetics of the exchange of  $\text{Li}^+$  between C222 and C221 and  $\gamma$ -butyrolactone as solvent, four solutions of different concentration ratio were prepared for each system. The concentration of lithium perchlorate in each solution was kept constant at 0.05 M, whereas the concentration of ligand was varied between 0.0175 M and 0.04 M. In this way the measurements were always performed in the presence of an excess of  $\text{Li}^+$ .

### $^7\text{Li}$ NMR spectroscopy

Variable-temperature and variable-pressure Fourier transform  $^7\text{Li}$  NMR spectra were recorded at a frequency of 155 MHz on a Bruker Avance DRX 400 WB spectrometer equipped with a superconducting BC-94/89 magnet system. Spinning tubes (5 mm) were used with a 1 mm o.d. melting point capillary inserted coaxially in the spinning tube and filled with an external reference solution (usually 1 M  $\text{LiClO}_4$  in DMF). The temperature dependence measurements were performed over a wide as possible temperature range for each system. A homemade high-pressure probe described in the literature [54] was used for the variable-pressure experiments, which were conducted at a selected temperature and at ambient, 30, 60, 90, 120 and 150 MPa pressure. A standard 5 mm NMR tube cut to a length of 45 mm was used for the sample solution. The

high-pressure NMR tube was sealed with a MACOR plug and an O-ring made of VITON. The plug and O-ring were shown to be stable in the employed solvent. The pressure was transmitted by the movable MACOR piston to the sample, and the temperature was controlled as described elsewhere [54]. For a typical kinetic run, 0.8 ml of solution was transferred under an Ar atmosphere to a Wilmad screw-cap NMR tube equipped with a poly(tetrafluoroethylene) septum. All test samples were prepared in the same way.

### Programs

The line widths of the NMR signals were obtained by fitting Lorentzian functions to the experimental spectra using the *NMRICMA 2.7* program [55] for Matlab [56]. The adjustable parameters were the resonance frequency, intensity, line width and baseline. Complete line-shape analysis based on the Kubo-Sack formalism using modified Bloch equations [57] was also performed with *NMRICMA 2.7* to extract rate constants from experimental spectra. The temperature and pressure dependent  $^7\text{Li}$  line widths and chemical shifts employed in the line shape analysis were extrapolated from low temperatures where no exchange-induced modification occurred.

### Quantum chemical calculations

All structures were optimized at the B3LYP/D95Vp hybrid DFT level [58–62] with no constraints other than symmetry and confirmed to be minima by computation of vibrational frequencies. Relative energies were corrected for zero point vibrational energy differences. The D95V basis set, augmented with polarisation functions (D95Vp), was used [63]. The Gaussian suite of programs was used throughout [64].

## Results and discussion

### Spectroscopic observation

In preliminary experiments, a series of  $^7\text{Li}$  NMR measurements for the  $\text{Li}^+$ -cryptand system in  $\gamma$ -butyrolactone as solvent were performed. For each of the cryptands C222, C221 and C211, mole ratio dependent measurements were performed by variation of both the cryptand: $\text{Li}^+$  and  $\text{Li}^+$ :cryptand molar ratios. The results enabled us to observe the distribution of particular species on increasing the amount of chelate or lithium salt. Basically, two signals of varying intensity were observed in the  $^7\text{Li}$  NMR spectra that refer to solvated  $\text{Li}^+$  and  $\text{Li}^+$  bound inside the cryptand cavity. In case of the smallest chelate C211, however, an additional signal appeared which can be ascribed to  $\text{Li}^+$  bound outside the cryptand and being partially solvated. The distribution plot for the various species in a solution of

C211 and  $\text{LiClO}_4$  in  $\gamma$ -butyrolactone is presented in Figure 3. The concentration of  $\text{LiClO}_4$  was kept constant at 0.01 M and the concentration of C211 was varied in the range 0–0.04 M. Initially only the signal of free (solvated)  $\text{Li}^+$  is observed, and then with increasing amount of C211, the signals referring to the complexed  $\text{Li}^+$  appear. Contrary to the larger cryptands, there are two signals that refer to bound  $\text{Li}^+$ ; one for  $\text{Li}^+$  inside the cavity and another of low intensity (max. 15%) for  $\text{Li}^+$  presumably bound outside the cryptand and being partially solvated. The latter signal, however, disappears once the C211/ $\text{LiClO}_4$  molar ratio gets to 1, and then all the  $\text{Li}^+$  is bound as internal complex. Due to the facts that the exchange process among the three species cannot be clearly defined,  $\text{Li}(\text{C211})^+$  is very stable and there is almost no exchange taking place, a detailed study of the observed rate constant,  $k_{\text{obs}}$ , for the exchange of  $\text{Li}^+$  as a function of temperature and pressure was undertaken only for C221 and C222. The lithium exchange reaction between cryptand and  $\gamma$ -butyrolactone was studied for four solutions with different ligand-to-metal ratios in the presence of an excess of  $\text{Li}^+$ .

Three signals can be observed in Figure S1 (Supporting Information); one comes from the reference (6.6 ppm) and the other two from the exchanging sites (6.0 ppm solvated  $\text{Li}^+$  and 4.8 ppm complexed  $\text{Li}^+$ ). At low temperature the signals are narrow and completely separated due to very slow or no exchange. Since the formation constant for  $\text{Li}(\text{C221})^+$  is very high [24], the concentration of bound lithium is equal to the amount of cryptand added. At ca. 358 K the signals start to coalesce and at 388 K only one broad signal (at 5.3 ppm) can be observed due to fast exchange. In the case of C222 (Figure S2, Supporting Information), the exchange process is faster due to the larger cavity of the cryptand. The signals that refer to solvated and complexed Li cation (8.3 ppm and 6.8 ppm, respectively at 218 K) coalesce at a lower temperature (ca. 268 K), and at high temperature (368 K) only one sharp signal at 7.7 ppm was

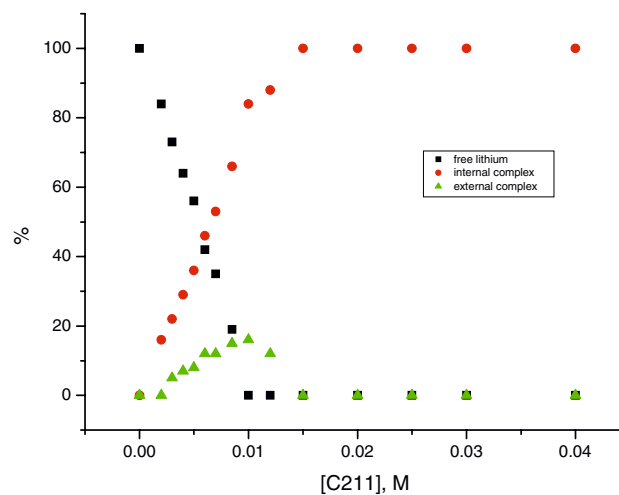


Figure 3. Distribution plot for various species in a solution of C211 and  $\text{LiClO}_4$  in  $\gamma$ -butyrolactone.

observed as a consequence of a very fast exchange process.

The rate of the exchange reaction increased not only with increasing cavity size of the cryptand but also with increasing concentration of the chelate, as can be recognized from the shape of the signals at 338 K in Figure 4 and from the values of  $k_{\text{obs}}$  in Table 1.

### Suggested exchange mechanism

As mentioned above, there are two possible mechanisms for the exchange of the lithium ion between the solvated and the complexed sites, namely bimolecular associative (I) and unimolecular dissociative (II) mechanisms.

At equilibrium:

$$\begin{aligned} k_1[*\text{Li}(\text{S})][\text{Li}(\text{L})] &= k_{-1}[*\text{Li}(\text{L})][\text{Li}(\text{S})] \\ k_2[\text{Li}(\text{S})][\text{L}] &= k_{-2}[\text{Li}(\text{L})][\text{S}] \end{aligned}$$

Therefore

$$-\frac{d}{dt}[\text{Li}(\text{S})] = k_{\text{obs}}[\text{Li}(\text{S})] = k_1[\text{Li}(\text{S})][\text{Li}(\text{L})] + k_{-2}[\text{Li}(\text{L})][\text{S}] \quad (1)$$

and

$$k_{\text{obs}} = k_1[\text{Li}(\text{L})] + \frac{k_{-2}[\text{Li}(\text{L})][\text{S}]}{[\text{Li}(\text{S})]} \quad (2)$$

An alternative form of Equation (2) is Equation (3), which was used to fit the data in Figures 5 and 7.

$$\frac{k_{\text{obs}}}{[\text{Li}(\text{L})]} = k_1 + k'_{-2} \frac{1}{[\text{Li}(\text{S})]} \quad (3)$$

Plots of  $k_{\text{obs}}/[\text{Li}(\text{L})]$  vs.  $1/[\text{Li}(\text{S})]$  were found to be linear with negligible slopes ( $k'_{-2} = k_{-2}[\text{S}]$ ) (especially at low temperature) and significant intercepts ( $k_1$ ) (see Figures 5 and 7). This indicates that the exchange mechanism has a more associative character for both

C221 and C222. This led us to take only the values of  $k_1$  into consideration, from which it follows that the exchange process is much faster for C222 than for C221. The corresponding Eyring plots for  $k_1$  are shown in Figures 6 and 8, respectively, and the thermal activation parameters are summarized in Table 2.

Based on the significantly negative activation entropy, the activation parameters support an associative interchange type of exchange process. Furthermore, the reported activation parameters are within the range of those reported by Popov and co-authors for closely related systems [31], viz.  $k_{298} = 680 \pm 42 \text{ M}^{-1} \text{ s}^{-1}$ ,  $\Delta H^\ddagger = 28 \pm 1 \text{ kJ mol}^{-1}$  and  $\Delta S^\ddagger = -101 \pm 2 \text{ J K}^{-1} \text{ mol}^{-1}$  for  $\text{Li}^+/\text{C221}$  in acetonitrile, and  $k_{298} = 892 \pm 50 \text{ M}^{-1} \text{ s}^{-1}$ ,  $\Delta H^\ddagger = 26 \pm 1 \text{ kJ mol}^{-1}$  and  $\Delta S^\ddagger = -109 \pm 2 \text{ J K}^{-1} \text{ mol}^{-1}$  for  $\text{Li}^+/\text{C221}$  in propylene carbonate, for which the authors also postulated an associative character for the  $\text{Li}^+$  exchange process. In the case of  $\text{Li}^+$  exchange between C222 and solvents such as acetonitrile, propylene carbonate and acetone, these authors found the mechanism to have more of a dissociative character. However, it should be pointed out that they used a different rate law than the one proposed by Shchori *et al.* [65] and that used in the present study, which complicates a direct comparison of the reported activation parameters with ours. It is reasonable to expect that solvents such as propylene carbonate, ethylene carbonate and  $\gamma$ -butyrolactone, together considered as a class of solvents that play an important role in polymer-gel lithium-ion batteries [66–70], due to their similar structure and properties as expected from their rather similar Gutmann donor numbers ( $DN = 15.1, 16.4$  and  $18.0$ , respectively [71]), should coordinate to  $\text{Li}^+$  in a similar way and should have a similar influence on the exchange mechanism. This observation corresponds to that reported by Shamsipur *et al.* [72] for the exchange of  $\text{Li}^+$  between C221 and acetonitrile–nitromethane mixtures. In all solvent mixtures used,  $\text{Li}^+$  exchange was found to occur via an associative mechanism, as expected for weak donor solvents ( $DN = 14.1$  and  $2.7$  for acetonitrile and nitromethane, respectively). The same group reported

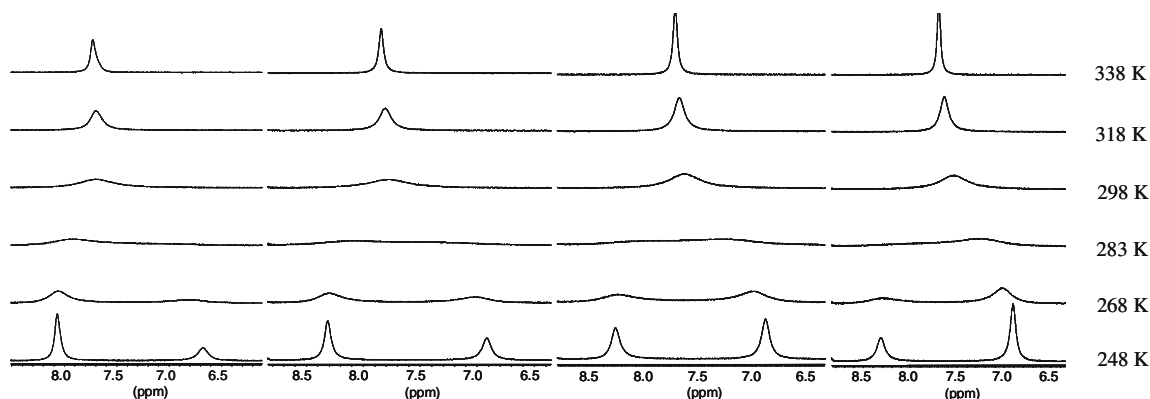


Figure 4.  $^7\text{Li}$  NMR spectra of C222 and  $\text{LiClO}_4$  in GBL. Temperature dependence for the sample ratios  $\text{C222}:\text{LiClO}_4 = 0.35, 0.45, 0.55$  and  $0.65$ .

Table 1. Values of the observed rate constants ( $k_{\text{obs}}$ ) calculated from the line shape analysis for the exchange of  $\text{Li}^+$  between solvated and chelated sites at 25 °C

Mole ratio C221: $\text{Li}^+$	$k_{\text{obs}}, \text{s}^{-1}$	Mole ratio C222: $\text{Li}^+$	$k_{\text{obs}}, \text{s}^{-1}$
0.4	$2.68 \pm 0.05$	0.35	$654 \pm 13$
0.5	$4.3 \pm 0.1$	0.45	$851 \pm 25$
0.65	$6.9 \pm 0.3$	0.55	$1282 \pm 51$
0.8	$9.6 \pm 0.5$	0.65	$1352 \pm 68$

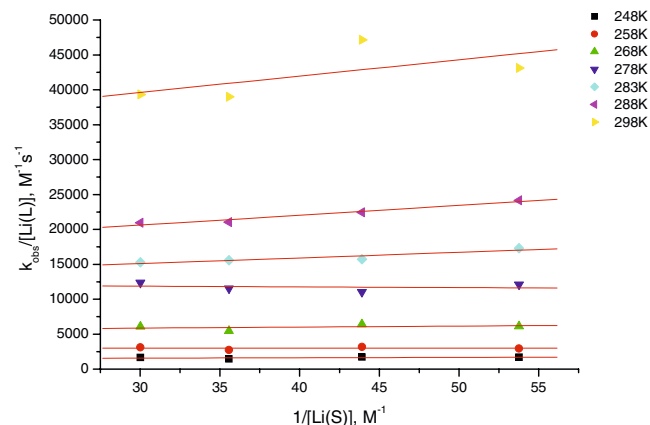


Figure 5. Plots of  $k_{\text{obs}}/[\text{Li(L)}]$  vs.  $1/[\text{Li(S)}]$  for C222 as a function of temperature.

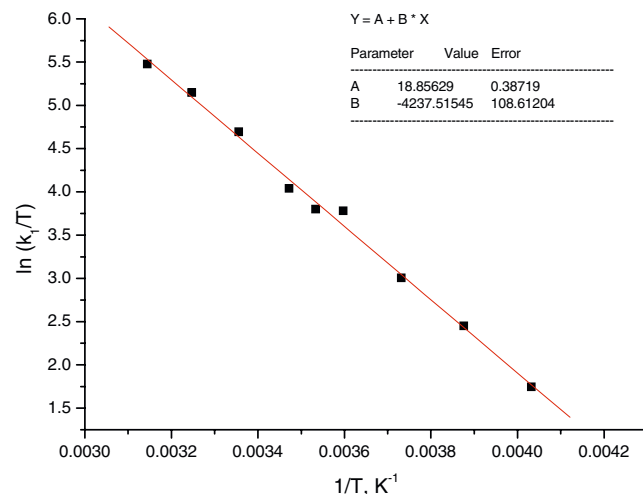


Figure 6. Eyring plot for  $k_1$  as a function of temperature for C222.

another case, where  $\text{Li}^+$  exchange occurred between C221 and mixtures of nitromethane (low donor ability) and dimethylformamide (high DN = 26.6), where it was found that the associative mechanism predominates in nitromethane, whereas a dissociative pathway prevails in dimethylformamide solution.

#### High pressure $^7\text{Li}$ NMR measurements

Additional mechanistic information on the intimate nature of the exchange mechanism can in principle be obtained from the effect of pressure on the  $\text{Li}^+$  exchange process [73–76]. A systematic pressure dependence study

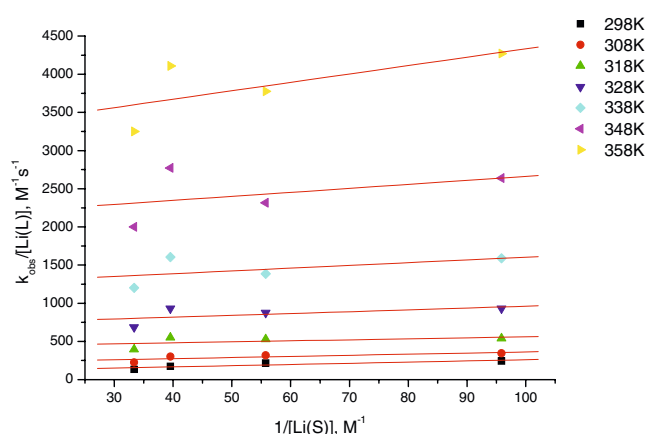


Figure 7. Plots of  $k_{\text{obs}}/[\text{Li(L)}]$  vs.  $1/[\text{Li(S)}]$  for C221 as a function of temperature.

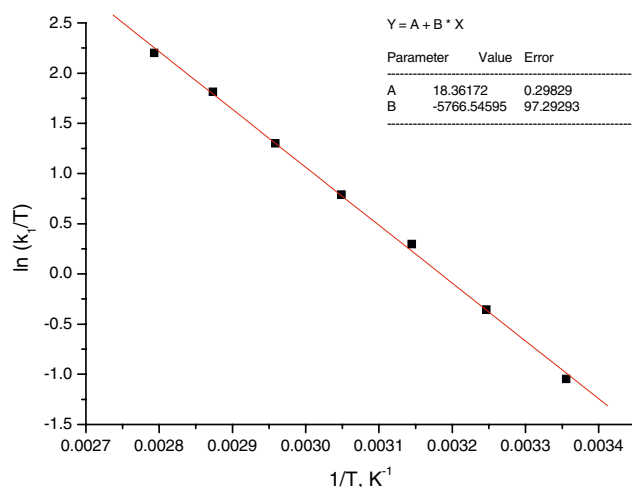


Figure 8. Eyring plot for  $k_1$  as a function of temperature for C221.

was performed to determine the volume of activation for the  $\text{Li}^+$  exchange process for both cryptates. Pressure dependent NMR spectra were recorded for each sample over the pressure range of 0.2–150 MPa at 316.5 K. The effect of pressure was found to be not very significant for these systems. There was a very small difference in the shape of the NMR spectra recorded at various pressures as can be seen in Figure S3 (Supporting Information). The rate constants calculated for each pressure were very similar within the experimental error limits and resulted in a practically zero value for  $\Delta V_{\text{obs}}^\ddagger$ , which points to a concerted interchange type of exchange mechanism [77]. In terms of an interchange mechanism, bond formation and bond cleavage occur in a concerted fashion without the formation of a distinct intermediate of higher or lower coordination number.

#### Influence of water

The rate of the exchange process was also investigated in a mixture of  $\gamma$ -butyrolactone and water in order to probe the impact of the solvent polarity and donor ability on the rate of the exchange reaction. The

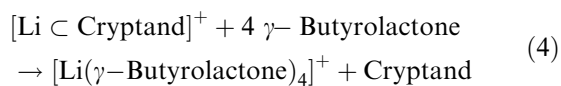
Table 2. Thermal activation parameters obtained from the values of  $k_1$  as a function of temperature

Chelate	$k_1^{298}$ , $M^{-1} s^{-1}$	$\Delta H^\ddagger$ , $kJ mol^{-1}$	$\Delta S^\ddagger$ , $J K^{-1} mol^{-1}$
C221	$105 \pm 32$	$48 \pm 1$	$-45 \pm 2$
C222	$(3.3 \pm 0.8) \times 10^4$	$35 \pm 1$	$-41 \pm 3$

exchange measurements were repeated for one of the samples (C222:LiClO<sub>4</sub> = 0.35) with 1  $\mu$ l H<sub>2</sub>O added to the 0.8 ml of  $\gamma$ -butyrolactone solution. It was observed that the exchange rate increased significantly as compared to the value obtained for the sample in the absence of water. The values of  $k_{obs}$  increase from 27 to 75 s<sup>-1</sup> at 248 K, from 654 to 1282 s<sup>-1</sup> at 298 K, and from 5945 to 12895 s<sup>-1</sup> at 358 K, on addition of water. This can be accounted for by the higher donor strength of water compared to  $\gamma$ -butyrolactone. It follows that the presence of water plays an important role in the exchange rate of Li<sup>+</sup> between cryptand and solvent.

#### Theoretical calculations

Experimentally a decrease in the cavity size hampers the exchange of Li<sup>+</sup> between the cryptand and the solvent. The improved binding of Li<sup>+</sup> in a smaller cavity should become visible from the structure and the following model reaction that describes the energy required for the dechelation process (Table 3).



It is noteworthy that in agreement with previous studies by Wipff and Wurtz [5], we also found only a limited flexibility for the investigated cryptands in our DFT calculations, justifying that all cryptands were calculated within the highest possible symmetry. In earlier work we demonstrated that Equation (4) is a valuable tool to determine ion selectivity as a function of the ionic radii [78]. We therefore examined the cavity size of the cryptands as a variable.

Table 4. Calculated (RB3LYP/D95Vp) and X-ray bond lengths (in Å)

d [Å]	C222	C221	C211	[Li(OH <sub>2</sub> ) <sub>4</sub> ] <sup>+</sup>	[Li( $\gamma$ -Butyrolactone) <sub>4</sub> ] <sup>+</sup>	[Li(NH <sub>3</sub> ) <sub>4</sub> ] <sup>+</sup>
Li-O	2.14	2.06–2.08	2.14	1.95	1.94	–
		2.10	2.11			
Li-N	2.22	2.28	2.38	–	–	2.13
PG	C <sub>3</sub>	C <sub>1</sub>	C <sub>2</sub>	T	C <sub>1</sub>	C <sub>1</sub>
X-ray		[79]	[80]	[81]		[82]
Li-O	–	1.99	2.17	1.96	–	–
		2.06	2.08			
		2.10				
Li-N	–	2.40, 2.44	2.29	–	–	2.08

In agreement with the experimental kinetic data, the smaller cryptand binds Li<sup>+</sup> better and slows down its exchange rate (Table 2). On comparing the calculated Li–O and Li–N bond lengths of the three structures with the bond distance in [Li(OH<sub>2</sub>)<sub>4</sub>]<sup>+</sup> and [Li(NH<sub>3</sub>)<sub>4</sub>]<sup>+</sup>, the trend can easily be understood (see Table 4 and Figure 9). In C222, Li<sup>+</sup> is four times weakly coordinated in a trigonal pyramidal shape by one Li–N and three Li–O interactions all clearly elongated (0.2 and 0.1 Å, respectively). The Li<sup>+</sup> cation in C221 is coordinated five times (distorted trigonal bipyramidal structure) by one nitrogen and four oxygen bonds all extended by around 0.15 Å. The coordinating bonds in [Li  $\subset$  C211]<sup>+</sup> are even more extended, but the Li–O bonds form a somewhat distorted tetrahedral coordination sphere for the lithium mono cation, while the stronger elongated Li–N bonds form a kind of second coordination sphere. Therefore, the lithium ion is formally six-coordinate. A comparison of the calculated and X-ray bond lengths shows a good agreement.

#### Conclusions

It can be concluded from the results of the present study that for the Li<sup>+</sup> exchange process between C222, C221 and  $\gamma$ -butyrolactone as solvent, two pathways, *viz.* bimolecular associative and unimolecular dissociative, compete with each other. The pressure dependence of the exchange process suggests the operation of a pure interchange mechanism, whereas the negative activation entropy values favor an associative interchange process. The basic idea of an interchange process involves concerted bond-formation and bond-cleavage, which is in agreement with the consideration that  $\gamma$ -butyrolactone is a rather weak donor. The results are in good agreement with that expected on the basis of a systematic comparison with data reported in the literature for solvents of similar donor strength.

Table 3. Dechelation energy,  $E_{dechelation}$ , for the reaction outlined in (4)

$\gamma$ -Butyrolactone	C222	C221	C211
$E_{dechelation}$ [kJ/mol]	–70.3	–48.6	–22.2

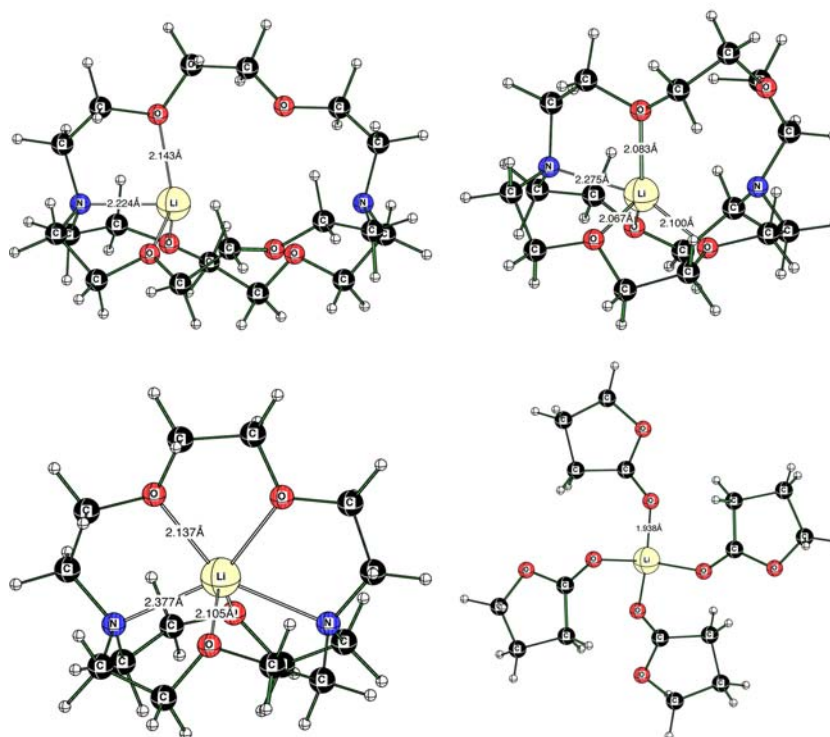


Figure 9. Optimized structures for  $[\text{Li} \subset \text{C222}]^+$ ,  $[\text{Li} \subset \text{C221}]^+$ ,  $[\text{Li} \subset \text{C211}]^+$  and  $[\text{Li}(\gamma\text{-Butyrolactone})_4]^+$ .

## Supporting Information

Ligand exchange processes on solvated lithium cations. II. Complexation by Cryptands in  $\gamma$ -Butyrolactone as Solvent<sup>+</sup>

Ewa Pasgreta, Ralph Puchta, Michael Galle, Nico van Eikema Hommes, Achim Zahl and Rudi van Eldik\*

**Electronic Supplementary Material** Supplementary material is available to authorised users in the online version of this article at <http://dx.doi.org/10.1007/s10847-006-9125-y>.

## Acknowledgements

This work was supported by the EC TMR network HPRN-CT-2000-19 (“Solvation Dynamics and Ionic Mobility in Conventional and Polymer Solvents”) and the Deutsche Forschungsgemeinschaft (SFB 583 on Redox-active Metal Complexes). We would like to thank Dr. Lothar Helm (EPFL Lausanne) for introducing E.P to *NMRICMA 2.7*, Prof. Walter Bauer for helpful discussions, Prof. Tim Clark for hosting this work in the CCC and the Regionales Rechenzentrum Erlangen (RRZE) for a generous allotment of computer time.

## References

1. B. Dietrich, J.M. Lehn, and J.P. Sauvage: *Tetrahedron Lett.* **34**, 2889 (1969).
2. B. Dietrich, J.M. Lehn, and J.P. Sauvage: *Tetrahedron Lett.* **34**, 2885 (1969).
3. J.M. Lehn: *Acc. Chem. Res.* **11**, 49 (1978).
4. J.M. Lehn: *Angew. Chem.* **100**, 91 (1988).
5. G. Wipff and J.M. Wurtz: *New J. Chem.* **13**, 807 (1989).
6. X.X. Zhang, R.M. Izatt, K.E. Krakowiak, and J.S. Bradshaw: *Inorg. Chim. Acta* **254**, 43 (1997).
7. J.M. Lehn and F. Montavon: *Helv. Chim. Acta* **59**, 1566 (1976).
8. R. Puchta, V. Seitz, N.J.R. van Eikema Hommes, and R.W. Saalfrank: *J. Mol. Model.* **6**, 126 (2000).
9. R.W. Saalfrank, A. Dresel, V. Seitz, S. Trummer, F. Hampel, M. Teichert, D. Stalke, C. Stadler, J. Daub, V. Schünemann, and A.X. Trautwein: *Chem. Eur. J.* **3**, 2058 (1997).
10. R.W. Saalfrank, V. Seitz, D.L. Caulder, K.N. Raymond, M. Teichert, and D. Stalke: *Eur. J. Inorg. Chem.* **9**, 1313 (1998).
11. R.W. Saalfrank, V. Seitz, F.W. Heinemann, C. Göbel, and R. Herbst-Irmer: *J. Chem. Soc., Dalton Trans.* **5**, 599 (2001).
12. B. Dietrich, J.P. Kintzinger, J.M. Lehn, B. Metz, and A. Zahidi: *J. Phys. Chem.* **91**, 6600 (1987).
13. L.F. Lindoy: *The Chemistry of Macrocyclic Ligand Complexes*, Cambridge University Press, Cambridge (1992), pp. 269.
14. M. Farahbakhsh, H. Schmidt, and D. Rehder: *Chem. Ber. Recl.* **130**, 1123 (1997).
15. C.E. Housecroft: *Cluster Compounds of Main Group Elements* (1996), p. 94.
16. M. Kirch and J.M. Lehn: *Angew. Chem.* **87**, 542 (1975).
17. J.M. Lehn and F. Montavon: *Helv. Chim. Acta* **61**, 67 (1978).
18. J.M. Lehn and J.P. Sauvage: *J. Chem. Soc., Chem. Commun.* **9**, 440 (1971).
19. W.E. Morf and W. Simon: *Helv. Chim. Acta* **54**, 2683 (1971).
20. M.J. Pregel and E. Buncel: *J. Am. Chem. Soc.* **115**, 10 (1993).
21. W. Simon, W.E. Morf, and P.C. Meier: *Struct. Bond.* **16**, 113 (1973).
22. K. Severin: *Coord. Chem. Rev.* **245**, 3 (2003).
23. R.H. Huang, M.J. Wagner, D.J. Gilbert, K.A. Reidy-Cedergren, D.L. Ward, M.K. Faber, and J.L. Dye: *J. Am. Chem. Soc.* **119**, 3765 (1997).
24. J.M. Lehn and J.P. Sauvage: *J. Am. Chem. Soc.* **97**, 6700 (1975).
25. G. Wipff and P. Kollman: *Nouv. J. Chim.* **9**, 457 (1985).
26. M. Shamsipur, E. Karkhaneei, and A. Afkhami: *Polyhedron* **17**, 3809 (1998).
27. Q. Chen, K. Cannell, J. Nicoll, and D.V. Dearden: *J. Am. Chem. Soc.* **118**, 6335 (1996).

28. M.K. Chantooni Jr. and I.M. Kolthoff: *J. Solution Chem.* **14**, 1 (1985).
29. B.G. Cox, J. Garcia-Rosas, and H. Schneider: *J. Am. Chem. Soc.* **103**, 1054 (1981).
30. R.R. Rhinebarger and A.I. Popov: *Polyhedron* **7**, 1341 (1988).
31. M. Shamsipur and A.I. Popov: *J. Phys. Chem.* **90**, 5997 (1986) and the references therein.
32. A.J. Smetana and A.I. Popov: *J. Solution Chem.* **9**, 183 (1980).
33. A. Abou-Hamdan and S.F. Lincoln: *Inorg. Chem.* **30**, 462 (1991).
34. P. Clarke, J.M. Gulbis, S.F. Lincoln, and E.R.T. Tiekink: *Inorg. Chem.* **31**, 3398 (1992).
35. P. Clarke, S.F. Lincoln, and E.R.T. Tiekink: *Inorg. Chem.* **30**, 2747 (1991).
36. S.F. Lincoln and A. Abou-Hamdan: *Inorg. Chem.* **29**, 3584 (1990).
37. S.F. Lincoln and T. Rodopoulos: *Inorg. Chim. Acta* **190**, 223 (1991).
38. S.F. Lincoln and T. Rodopoulos: *Inorg. Chim. Acta* **205**, 23 (1993).
39. S.F. Lincoln and A.K.W. Stephens: *Inorg. Chem.* **30**, 3529 (1991).
40. A.K.W. Stephens, R.S. Dhillon, S.E. Madbak, S.L. Whitbread, and S.F. Lincoln: *Inorg. Chem.* **35**, 2019 (1996).
41. R.M. Izatt, K. Pawlak, J.S. Bradshaw, and R.L. Bruening: *Chem. Rev.* **91**, 1721 (1991).
42. E. Shchori, J. Jagur-Grodzinski, and M. Shporer: *J. Am. Chem. Soc.* **95**, 3842 (1973).
43. B.O. Strasser, K. Hallenga, and A.I. Popov: *J. Am. Chem. Soc.* **107**, 789 (1985).
44. B.O. Strasser and A.I. Popov: *J. Am. Chem. Soc.* **107**, 7921 (1985).
45. R.M. Izatt, J.S. Bradshaw, S.A. Nielsen, J.D. Lamb, J.J. Christensen, and D. Sen: *Chem. Rev.* **85**, 271 (1985).
46. R.M. Izatt, J.S. Bradshaw, K. Pawlak, R.L. Bruening, and B.J. Tarbet: *Chem. Rev.* **92**, 1261 (1992).
47. R.M. Izatt, K. Pawlak, J.S. Bradshaw, and R.L. Bruening: *Chem. Rev.* **95**, 2529 (1995).
48. K. Sonoda, M. Deguchi, H. Koshina, M. Armand, C. Michot, and M. Gauthier: *Proc. Electrochem. Soc.* **2002-26**, 512 (2003).
49. N. Takami, M. Sekino, T. Ohsaki, M. Kanda, and M. Yamamoto: *J. Power Sources* **97-98**, 677 (2001).
50. H.M.R. Hoffmann and J. Rabe: *Angew. Chem.* **97**, 96 (1985).
51. S.K. Mandal, S.R. Amin, and W.E. Crowe: *J. Am. Chem. Soc.* **123**, 6457 (2001).
52. Y.-L. Zhu, H.-W. Xiang, G.-S. Wu, L. Bai, and Y.-W. Li: *Chem. Commun.* **3**, 254 (2002).
53. M. Masia and R. Rey: *J. Phys. Chem. B* **108**, 17992 (2004).
54. A. Zahl, A. Neubrand, S. Aygen, and R. van Eldik: *Rev. Sci. Instrum.* **65**, 882 (1994).
55. L. Helm and A. Borel: *NMRICMA 2.7*, University of Lausanne (2000).
56. Matlab: version 5.3.1., Mathworks Inc., (1999).
57. J.A. Pople, W.G. Schneider, and H.J. Bernstein: *High-Resolution Nuclear Magnetic Resonance*. McGraw-Hill Book Company, Inc., (1959), p. 513.
58. A.D. Becke: *J. Chem. Phys.* **98**, 5648 (1993).
59. C. Lee, W. Yang, and R.G. Parr: *Phys. Rev. B., Condens. Matter Mater. Phys.* **37**, 785 (1988).
60. P.J. Stephens, F.J. Devlin, C.F. Chabalowski, and M.J. Frisch: *J. Phys. Chem.* **98**, 11623 (1994).
61. T.H. Dunning Jr. and P.J. Hay: *Modern Theoretical Chemistry*, Plenum, New York (1976), pp. 1.
62. S. Huzinaga, J. Andzelm, M. Klobukowski, E. Radzio-Andzelm, Y. Sakai, and H. Tatewaki: *Gaussian Basis Sets for Molecular Calculations*, Elsevier, Amsterdam (1984).
63. The performance of the computational level employed in this study is well documented, see for example: P. Illner, A. Zahl, R. Puchta, N. van Eikema Hommes, P. Wasserscheid, and R. van Eldik: *J. Organomet. Chem.* **690**, 3567 (2005); S. Klaus, H. Neumann, H. Jiao, A. Jacobi von Wangelin, D. Goerdes, D. Struebing, S. Huebner, M. Hateley, C. Weckbecker, K. Huthmacher, T. Riermeier, and M. Beller: *J. Organomet. Chem.* **689**, 3685 (2004); R.W. Saalfrank, C. Deutscher, H. Maid, A.M. Ako, S. Sperner, T. Nakajima, W. Bauer, F. Hampel, B.A. Hess, N.J.R. van Eikema Hommes, R. Puchta, and F.W. Heinemann: *Chem. Eur. J.* **10**, 1899 (2004); A. Scheurer, H. Maid, F. Hampel, R.W. Saalfrank, L. Toupet, P. Mosset, R. Puchta, and N.J.R. van Eikema Hommes: *Eur. J. Org. Chem.* **12**, 2566 (2005); C.F. Weber, R. Puchta, N.J.R. van Eikema Hommes, P. Wasserscheid, and R. van Eldik: *Angew. Chem.* **117**, 6187 (2005); C.F. Weber, R. Puchta, N.J.R. van Eikema Hommes, P. Wasserscheid, and R. van Eldik: *Angew. Chem. (Int. ed. Eng.)* **44**, 6033 (2005).
64. M. J. Frisch, G.W. Trucks, H.B. Schlegel, G.E. Scuseria, M.A. Robb, J.R. Cheeseman, J.A. Montgomery Jr., T. Vreven, K.N. Kudin, J.C. Burant, J.M. Millam, S.S. Iyengar, J. Tomasi, V. Barone, B. Mennucci, M. Cossi, G. Scalmani, N. Rega, G.A. Petersson, H. Nakatsuji, M. Hada, M. Ehara, K. Toyota, R. Fukuda, J. Hasegawa, M. Ishida, T. Nakajima, Y. Honda, O. Kitao, H. Nakai, M. Klene, X. Li, J.E. Knox, H.P. Hratchian, J.B. Cross, V. Bakken, C. Adamo, J. Jaramillo, R. Gomperts, R.E. Stratmann, O. Yazyev, A.J. Austin, R. Cammi, C. Pomelli, J.W. Ochterski, P.Y. Ayala, K. Morokuma, G.A. Voth, P. Salvador, J.J. Dannenberg, V. G. Zakrzewski, S. Dapprich, A.D. Daniels, M.C. Strain, O. Farkas, D.K. Malick, A.D. Rabuck, K. Raghavachari, J.B. Foresman, J.V. Ortiz, Q. Cui, A.G. Baboul, S. Clifford, J. Cioslowski, B.B. Stefanov, G. Liu, A. Liashenko, P. Piskorz, I. Komaromi, R.L. Martin, D.J. Fox, T. Keith, M.A. Al-Laham, C.Y. Peng, A. Nanayakkara, M. Challacombe, P.M.W. Gill, B. Johnson, W. Chen, M.W. Wong, C. Gonzalez, and J.A. Pople: *Gaussian 03, Revision B.03*, Gaussian Inc., Wallingford, CT (2004).
65. E. Shchori, J. Jagur-Grodzinski, Z. Luz, and M. Shporer: *J. Am. Chem. Soc.* **93**, 7133 (1971).
66. J.Y. Song, Y.Y. Wang, and C.C. Wan: *J. Power Sources* **77**, 183 (1999).
67. Y. Matsuda, T. Fukushima, H. Hashimoto, and R. Arakawa: *J. Electrochem. Soc.* **149**, A1045 (2002).
68. J. Adebahr, M. Forsyth, D.R. MacFarlane, P. Gavelin, and P. Jacobsson: *J. Mater. Chem.* **13**, 814 (2003).
69. M.S. Ding, K. Xu, J.P. Zheng, and T.R. Jow: *J. Power Sources* **138**, 340 (2004).
70. M. Ue: *J. Electrochem. Soc.* **141**, 3336 (1994).
71. Y. Marcus: *Chem. Soc. Rev.* **22**, 409 (1993).
72. M. Shamsipur, E. Karkhaneei, and A. Afkhami: *J. Coord. Chem.* **44**, 23 (1998).
73. A.V. Davis, D. Fiedler, G. Seeber, A. Zahl, R. van Eldik, and K.N. Raymond: *J. Am. Chem. Soc.* **128**, 1324 (2006).
74. R. van Eldik and C.D. Hubbard: *Chemistry at Extreme Conditions*, Elsevier, Amsterdam (2005), pp. 109.
75. M. Wolak and R. van Eldik: *J. Am. Chem. Soc.* **127**, 13312 (2005).
76. A. Zahl, R. van Eldik, M. Matsumoto, and T.W. Swaddle: *Inorg. Chem.* **42**, 3718 (2003).
77. L. Helm and A.E. Merbach: *Chem. Rev.* **105**, 1923 (2005).
78. M. Galle, R. Puchta, N.J.R. van Eikema Hommes, and R. van Eldik: *Z. Phys. Chem.* **220**, 511 (2006).
79. S. Choua, H. Sidorenkova, T. Berclaz, M. Geoffroy, P. Rosa, N. Mezailles, L. Ricard, F. Mathey, and P. Le Floch: *J. Am. Chem. Soc.* **122**, 12227 (2000).
80. D. Moras and R. Weiss: *Acta Crystallogr., Sect. B: Struct. Crystallogr. Cryst. Chem.* **29**, 400 (1973).
81. W. Meske and D. Babel: *Z. Anorg. Allg. Chem.* **624**, 1751 (1998).
82. N. Scotti, U. Zachwieja, and H. Jacobs: *Z. Anorg. Allg. Chem.* **623**, 1503 (1997).